#3934

HI-85-11 No. 1

Comparisons of Four Computer Models with Experimental Data from Test Buildings in Northern New Mexico

D.K. Robertson, P.E. J.E. Christian
ASHRAE Associate Member

ABSTRACT

Eight one-room test buildings, 20 ft (6.1 m) square and 7.5 ft (2.3 m) high, were constructed on a high desert site near Tesuque Pueblo, New Mexico, to study the influence of wall dynamic heat transfer characteristics on building heating energy requirements (the "thermal mass effect"). The buildings are nominally identical except for the walls (adobe, concrete and masonry unit, wood-frame, and log) and are constructed so as to isolate the effects of the walls. The amount of mass in the walls varies from 240 lb/ft^2 (1171 kg/m^2) for the 2 ft (.61 m) thick adobe wall to 4.3 lb/ft^2 (21 kg/m^2) for the insulated wood-frame wall. The roof, floor, and stem walls are all well insulated and the buildings were constructed with infiltration rates less than 0.4 air change per hour. The site is instrumented to record building component temperatures and heat fluxes, outside weather conditions, and heating energy use. Data were collected for two heating seasons from midwinter to late spring with the buildings in two configurations, with and without windows.

Four computer codes were used to simulate the performance of the test buildings without windows, using site weather data. The codes used were DOE-2.1A, DOE-2.1C, BLAST, and DEROB. Each code was run by a different analyst. Simulations were done for midwinter, late winter, and spring. Two of the test cell comparisons are discussed; the insulated frame and an 11-in (.28 m) adobe.

This work presents a quantitative and qualitative critical comparison of the modeling and experimental results. Cumulative heating loads, wall heat fluxes, and air and surface temperatures are compared, as well as input assumptions to the models. Explanations of differences and difficulties encountered are reported. The principal findings were that cumulative heating loads and the characteristic influences of wall thermal mass on hourly behavior were reproduced by the models.

INTRODUCTION

This paper summarizes five major work efforts: an experimental study and four computer modeling efforts. The experimental study, called the Southwest Thermal Mass Study (SWTMS), was performed at Tesuque Pueblo, New Mexico. Its purpose was to evaluate the effect of envelope thermal mass on the heating energy consumption of conventional (nonsolar) residential buildings. A parallel experiment, which also included cooling, was performed at the National Bureau of Standards.

*Research sponsored by U.S. Department of Energy under contract No. DE-AC05-840R21400 with Martin Marietta Energy Systems, Inc., as part of the National Program for Building Thermal Envelope Systems and Materials.

David K. Robertson, New Mexico Energy Research and Development Institute, 457 M Washington, S.E., Albuquerque, NM 87108.

Jeffrey E. Christian, Energy Division, Oak Ridge National Laboratory, Oak Ridge, TN 37831.

CONTENTS

The experimental work was performed by the State of New Mexico's Energy Research and Development Institute at the University of New Mexico under subcontract with Oak Ridge National Laboratory. The experimental design, results, and analysis are contained in a series of three reports (Gustinis and Robertson 1981; Gustinis and Robertson 1984; Robertson 1984). The work was done as part of the Department of Energy's Thermal Mass Program, which has as a major objective a reliable and accurate data and analysis base, derived from experimental measurements, that offers an opportunity for building owners to use mass more effectively (Courville and Christian 1983).

The thermal mass field data will be used in the development and support of building energy use codes, in the development of simplified design tools, and in the validation of computer building simulation models, along with a host of other building research activities. At present, the simplified predictive tools proposed for estimating the effect of mass are not at all agreed upon by some sectors of the building industry, in particular those that produce high mass products, such as concrete, masonry, logs, and adobe units, and those that provide light mass products, such as insulation.

Credibility of the raw data was considered paramount. To enhance the quality and reliability of the data beyond the execution of good experimental technique, four independent studies were initiated with the objective of performing consistency checks on the data. The primary foci were internal consistency of measured data and agreement of measured data with theory, as written into large main-frame building thermal models. No extensive attempt was made to validate analysis, only the data. If the data are high quality, accurate, and scrutinized by many, the opportunity of conducting credible analysis of the effect of thermal mass, with the data as the foundation, greatly increases.

The four modeling efforts discussed are: DOE-2.1A by Dr. Howard McLain et al. of Oak Ridge National Laboratory (ORNL) (1984); BLAST by Bill Carroll et al. of Lawrence Berkeley Laboratory (LBL) (undated); DEROB by Dr. Francisco Arumi-Noe of the University of Texas (1984); and DOE-2.1C by Bruce Birdsall of LBL (1985). The experimental work was performed in 1982 and 1983; the modeling work was done in 1983 and 1984. This paper describes the experimental effort in some detail and then describes the different approaches used and the results obtained by each of the four modeling efforts. Despite the variation of approaches, cumulative predictions of heating loads for one- to two-week periods were generally within 10% of the experimental sums. The models tended to be more accurate in predicting the one-dimensional heat flow at the center of each wall. The computer models also support the conclusions of the experiment concerning the order of magnitude and mechanisms of operation of the thermal mass effect.

THE SOUTHWEST THERMAL MASS STUDY

The Southwest Thermal Mass Study is a research facility at Tesuque Pueblo, New Mexico, designed to address the effects of envelope thermal mass on building energy performance in the sunny climate of the American Southwest. The study uses a traditional material, sun-dried adobe brick, as the primary material for study of mass effects. In addition to five adobe test buildings, there is a concrete masonry building, another of milled logs, and one of insulated wood-frame construction, providing eight fully-instrumented test buildings with walls of different thicknesses, densities, and thermal diffusivities.

The test facility is located in a high desert valley at an altitude of 6330 ft (1930 m), at 35.8 degrees north latitude and 107.0 degrees west longitude, on Tesuque Pueblo land 9 miles (15 km) north of Santa Fe, New Mexico. The winter climate is characterized by 5760 ± 400, (65 F base temperature) (3200 ± 220 - SI, 18.3°C base temperature) heating degree days. Insolation is high: over 65% of the extraterrestrial solar radiation flux reaches the test site. The insolation during the day, combined with the clear night skies, produces typical diurnal air temperature swings of 27 to 36 F (15 to 20°C). Exterior surfaces of insulated walls exposed to the sun can experience diurnal temperature swings over 100 F (55°C) on windless days. Wind speeds at nearby Santa Fe average 12 mph (19 km/h) at 33 ft (10 m) height.

The eight windowless test buildings were nearly identical in construction, except for their exterior walls. A picture of one of the test buildings is shown in Figure 1. They are 20 ft (6.1 m) square and 7.5 ft (2.3 m) high inside, except that the insulated wood-frame building is 20.7 ft (6.3 m) square with 8.0 ft (2.4 m) ceilings. The floors are 4 in (.10 m) concrete slab-on-grade, with 2.0 in (.05 m) of aluminum-faced polyisocyanurate or polyurethane foam insulation placed over the concrete to insulate it from the interior. Concrete stem walls reaching 2.0 ft (0.6 m) deep are insulated on both sides with 2.0 in (.05 m) of urethane foam.

The stem walls vary in thickness with the walls they support. Flat roofs cover the buildings. They are supported by 2 x 12 (.04 m by .29 m) wood joists on 16 in (.41 m) centers, with spaces filled by glass fiber batt insulation. A polyethylene vapor and infiltration barrier and 1/2 in (.01 m) gypsum board finish the ceiling. There are neither doors nor windows: a weatherproof roof entrance provides access.

The heating plant in each building consists of three 5120 Btu/h (1500 W) electrical resistance heaters controlled by a thermostat. Building air is mixed by a 290 ft ^{3}/min (0.14 m^3/s) fan blowing downward through a centrally located 2 ft ^{2} (0.61 m ^{2}) destratification plenum. The thermostat is located within the plenum, and heaters are dispersed around the plenum base, as shown in Figure 1.

The test building instrumentation consisted of each wall of each building being instrumented to measure surface and interior temperatures and interior surface heat flux. The roofs were of light construction, and identical, so interior and exterior roof surface temperatures were measured in one building only, to determine roof properties. During most of the year, floor slab temperatures were measured below the 2.0 in (.05 m) insulation for one building only and heat flows were calculated from the insulation R-value and imposed temperature difference.

Inside each test building, air temperatures were measured in the plenum near the thermostat, at mid-height 1.0 ft (.31 m) from each wall, and 1.0 ft (.31 m) from the floor and ceiling. A globe temperature was measured at midheight near the north wall. Measurements of outdoor air temperature, wind speed and direction, relative humidity, barometric pressure, solar flux on a horizontal plane and on cardinally oriented vertical planes, direct-normal solar flux, and long-wave flux on a horizontal surface defined the outdoor conditions. Some ground temperature measurements were also taken. Measurements of solar absorptance of test building walls, test building infiltration rates, infrared imaging system scans of the buildings to check for inhomogeneities and construction flaws, and other tests were performed as necessary.

Analysis of the experimental data consisted of checks for consistency in the data, qualitative observations on how the envelope thermal mass affects annual energy consumption, and estimation of the annual effect. The principal check for consistency was an energy balance for each building for selected five-day periods throughout the heating season. In most cases, the sums of measured heat loss were within 10% of the measured heating energy consumption (see Figures 2 and 3).

It was found that the mass effect can save heating energy as follows. If heating is required continuously, the stored (and subsequently released) heat in the envelope mass has no effect on the building's heating load. That is, the average heating requirement is the same as that of a less massive building with the same insulating characteristics. This is what occurs in midwinter in northern New Mexico. However, when the interior temperature tends to float above the thermostat set point for part of the day (as in spring and fall in northern New Mexico), the ability of massive walls to store and release heat on a diurnal basis reduces the building's heating energy consumption, in comparison with a less massive building with the same insulating characteristics. In effect, the more massive building puts a more constant load on the building's heating plant. This reduces both the amount of temperature floating above the thermostat set point during the day and the heating load at night.

Figure 4 is a plot of SWTMS data that shows how the SWTMS data has been analyzed. The ordinate is the heating load of a lightweight building (2 in x 4 in [.04 m x .09 m] wood-frame), and the abcissa is the heating load of a massive reference case (14-in [.36 m] adobe). Each point represents a five-day period, and the points are spread over a heating season. During colder weather, at the upper end of the curve, the lightweight building has a heating load proportional to the massive building. During warmer weather, at the lower end of the curve, however, the lightweight building has a higher heating load in proportion to the massive building.

A plot similar to this, called the "signature" of the building, was produced for each test building. The signatures can be used to estimate the annual mass effect, as follows. The signature is a correlation of a building's heating load with that of a massive reference building. The massive reference building, it was found, represents the steady-state prediction using average data, in which average U-values and weekly average weather data are used. The heating load of the reference building (the steady-state prediction) can be calculated, and the heating load of the building in question then can be calculated.

This experimentally derived methodology was applied to all test buildings for two heating seasons for two locations in New Mexico — Santa Fe, near the test site, and Las Cruces, a warmer location than the test site. It was found that the maximum effect for windowless test buildings on an annual basis for the lightweight building was on the order of 2% to 4%. The variation depended on the relative amount of moderate weather versus cold weather, with the warmer weather (e.g., warmer climate or less severe heating season) showing a greater effect.

The maximum effect observed at the site after windows were added was around 5%. Using the predictive procedure described above, the maximum predicted effect for Las Cruces, with almost half the heating degree days as the site, was near 12% (Robertson 1984), although the absolute effects in terms of energy use were similar.

THE MODELING EFFORT

General Considerations

The four models used were DOE-2.1A, DOE-2.1C, BLAST, and DEROB. The DOE-2 computer programs use building construction and geometry data together with hourly weather data to predict the dynamic thermal behavior of the building (McLain et al. 1984). One-dimensional heat flow is assumed for all building surfaces, as is the case for the other two models used. For the massive surfaces exposed to the atmosphere, the programs account for the delay of heat transfer by the use of response factors. (The response factor method describes the heat flow through a wall due to a unit temperature difference pulse between the wall surfaces.) The programs use the weighting factor method to calculate the heating loads in each zone of a building, assuming fixed zone temperatures. They then use the weighting factor method again to modify the loads calculated at the fixed zone temperatures to calculate the hourly zone temperatures and the heating system energy output.

Other than the specific input assumptions and data used, the handling of these two types of heat transfer (at the exterior walls and within the zone) are the two most important differences between DOE-2 and the other computer models. The changes within DOE-2.1 between versions A and C do not change the results of modeling these test cells. However, the input files vary, primarily by selecting two different methods for modeling the thermostat behavior.

The BLAST computer model also uses a response factor method to calculate heat transfer through exterior walls. However, the heat transfer within the interior of a building to the inside surface of an exterior wall is handled differently, using an explicit method. In this method, the path of heat flow from interior air to exterior air is assigned a series of nodes, each of which has a temperature at the beginning of the time increment (usually hourly). An equation is written stating the conductive, convective, and radiative relationship between each directly communicating pair of nodes, as well as the heat storage at each node. All energy balance equations are then solved simultaneously to determine the new temperatures at the nodes at the end of the hour.

The DEROB simulation model uses explicit, nodal energy balance methods to calculate the heat transfer at the wall and at the interior.

All four models have the capability to output the values of key parameters on an interval (hourly) or cumulative basis. For this study, the important parameters were: interior air temperature, wall heat flux, and heating energy use. All three are important with respect to the effects of thermal mass. Interior air temperature floating is a critical factor in the "thermal mass effect." Wall heat flux reflects the presence or absence of dynamic thermal storage effects in exterior walls. And, of course, the "bottom line" was: how much energy savings from envelope thermal mass do the models predict, compared to the experimental data?

A major portion of any modeling effort is to accurately characterize the actual physical situation of the building being modeled. This includes both driving parameters, such as weather, and the thermophysical properties of the structures. Figure 5 is a simplified schematic representation of the heat loss of the test buildings. Temperature nodes are represented by dots and the letters "T," and the coupling between nodes (the thermal resistance to heat transfer) are represented by the electrical symbols for resistance and the letters "R." Heat gains are represented by the letters "Q."

Heat is generated by the heating system at the plenum. It is then transferred, primarily through forced and natural convection, to the outer "zone" of the building. That outer zone communicates with the outside air through the walls, the roof, infiltration, and floor edge

losses, as well as with the ground through center floor losses. Internal loads, in this case only fan energy in the heating system, are added directly to the plenum air or the room air, and solar energy is added to the room space via the walls for these windowless units.

It is the job of the modeler to accurately quantify each T, R, and Q. These are the input data to the model. Table 1 gives the input assumptions for each of the four sets of models. Parameters 1 through 4 characterize the relationship between the plenum air temperature and the room air temperature and are the most widely varying set of parameters for the four models. They effectively characterize the "interzone R-value" between the two nodes. A major complication in modeling these small 20 ft (6.1 m) by 20 ft (6.1 m) test buildings is that the air temperature is horizontally stratified. This is particularly true for the uninsulated adobe buildings and more so in the winter periods than in the spring, as shown by Figure 6.

It is clear from the variation in these model input assumptions that the relationship between the heating system and the room air is complex, even for such conceptually simple parameters as room air temperature and thermostat setpoint. These input assumptions are perhaps the most important for successful modeling of these structures.

Parameters 5 through 9 in Table 1 characterize the heat transfer of the walls. Varying assumptions were made for interior and exterior surface film coefficients, and the three wall material properties of surface-to-surface thermal resistance, density, and heat capacity. In addition, all modelers assumed that the time lag of the flux response to the exterior sol-air pulse was as experimentally measured. A major difference was the characterization of the adobe walls: DOE-2 was programmed to use the same values that were measured experimentally, but the other two models used a much smaller density, and DEROB used an adobe wall R-value 50% higher than the experimentally measured value. The DEROB simulations were run with two sets of thermophysical values for adobe. The set reported on in this paper came from the DEROB wall library and produced unrehearsed outputs. The results shown are first attempts, not values obtained after calibration. A second set used the thermophysical properties measured by Gustinis and Robertson, and the DEROB runs overpredicted the adobe heating load by about 35% (Arumi-Noe 1984).

The remaining parameters shown in Table 1 complete the description of the thermal network. In most cases, the models had similar assumptions: the infiltration model was that derived experimentally; the weather data (primarily outside temperature and solar radiation) was actual site data; the internal loads were as measured; and the roof R-values were similar. The slab-on-grade floors are perhaps the single building envelope element that we know least about thermally. More than in any other element, there is three-dimensional heat transfer, and there is thermal communication with the diurnally varying outside air and surface ground, as well as the annually varying deep ground. The input parameter differences and output parameter comparisons are discussed further in the following section.

Approach

Each of the four modelers was asked to look for data consistency both internally and with outputs from mainframe building simulation models. The same building performance and site weather data bases were given to each, and no other modeling constraints were imposed. The four modelers used four different approaches. Three of the analysts chose to simulate the test buildings using a single-zone model except for Arumi-Noe who input a two-concentric-zone model.

DEROB. In Arumi-Noe's model, the inner zone represents the plenum, which is treated as a conditioned space. The outer zone represents the remainder of the test building and is coupled to the inner via natural and forced convection, as well as infrared radiation and conduction through the plywood walls of the plenum. The thermostat in the conditioned space was set at 69.1 F (20.6°C). Whenever the plenum temperature went below this value, the heater comes on to bring the plenum temperature to the value. The outer zone temperature floats according to the energy balance controlling the unconditioned space. The horizontal temperature stratification followed naturally from the two-zone model.

DOE-2.1A. Since the measured data strongly suggest horizontal temperature stratification, and DOE-2.1A restricts single zone models to having a uniform temperature, a multiple zone model was attempted at first to permit different temperatures within the test cell. The difficulty with this approach in DOE-2.1 was that the allocation of the air flowing from the heaters into the different zones and the exchange of heat between the different zones had to be estimated by trial and error. Therefore, this technique was abandoned in favor of a single-zone model in which the thermostat set point was modeled by a regression of the daily average air temperature near the walls with the daily average heating energy use rate.

BLAST. An attempt to utilize the same methodology used in DOE-2.1A described above (that is, time-varying air temperatures measured near the cell walls as the interior control temperature) was abandoned because this approach in BLAST yielded no reasonable results (Carroll et al. undated).

This brought into question the accuracy of the air-temperature measuring thermocouples near the walls and led to examination of the literature on experimental and theoretical work on turbulent natural convection that discusses the development of the thermal boundary layer for simple systems. Based on the assumption that the test cells behaved in a similar fashion as the simple test apparatus, which measures heat transfer in the water layer confined by two horizontal plates, heated from below and cooled from above, it was concluded that: (1) The air is a uniform temperature and there is a region very close to the external wall in which the sudden changes in temperature occur (Carroll et al. undated). This region is called thermal boundary layer. (2) The zonal air temperatures were measured one foot away from the walls, which lies in the well-mixed region (uniform temperature region) and is outside the thermal boundary layer for simple systems under the turbulent natural convection flow conditions (Carroll et al. undated). In the experimental data, the air temperature measurements vary considerably; therefore, the measurements are believed by the BLAST modelers to be in error and are ignored.

The measured hourly plenum temperatures averaged over each simulation period were used as the thermostat control temperature in all BLAST simulations. The floating range was kept to 0.02 F (0.011°C) and the thermostat set point varied for each of the three simulated periods to coincide with the different measured averages.

DOE-2.1C. The modeling approach selected by Bruce Birdsall of LBL, using DOE-2.1C, was to use a single zone with a constant setpoint of 64 F (17.8°C) (the lowest observed space temperature), combined with a throttling range of +5 F (2.78°C). It was felt that the reason for the discrepancy between the measured space temperature one foot away from the external walls and the plenum temperature was primarily due to thermostat droop and conforms with the regression equation used by McLain in DOE-2.1A.

Specific Parameters

Wall Interior — Surface Film Coefficient. DOE-2.1 uses a constant 1.47 Btu/h $\cdot$ft$^2\cdot$F (8.35 W/h$\cdot$m$^2\cdot$°C) heat transfer coefficient, which includes 0.8 Btu/h $\cdot$ft$^2\cdot$F (4.54 W/h $\cdot$m$^2\cdot$°C) for the radiation coefficient of the walls. BLAST uses a constant 0.54 Btu/h $\cdot$ft$^2\cdot$F (3.07 W/h$\cdot$m$^2\cdot$°C) for the convective component and calculates the radiative fraction based on other surface temperatures seen by each wall. DEROB calculates the heat transfer coefficient on both sides of the wall each hour. The values depend on the surface temperatures, air velocity, air temperature, and surface tilt angle.

Wall Exterior - Surface Film Coefficient. BLAST and DOE-2.1 both use a simple algorithm to calculate the exterior surface heat transfer coefficient as a function of wind speed. For example, at 10 mph, the value is 4.2 Btu/h $\cdot$ft$^2\cdot$F (23.8 W/h $\cdot$m$^2\cdot$°C).

Surface-to-Surface R-Value. The DOE-2.1 and BLAST runs both used conductivity values measured experimentally for both the frame and adobe test cells, although there were some small differences as shown in Table 1. The major difference is that the DEROB runs used a wall R-value about 50% larger than the experimentally determined value of around 2 h $\cdot$ft$^2\cdot$F/Btu (0.35 h$\cdot$m$^2\cdot$°C/W). Additional DEROB runs using the same conductivity values used in DOE-2.1 and BLAST produced loads 35% above measured values.

Wall Density. All the thermophysical wall properties were measured except specific heat. DOE-2.1 used the experimentally measured 117 lb/ft^3 (1874 kg/m^3). BLAST and DEROB both used the lower values of 80 and 90 (1281 and 1441 kg/m^3), respectively. An adobe block left over from the test cell construction that had been sitting in an office in New Mexico for four years was reweighted at 112 lb/ft^3 (1800 kg/m^3).

Other. There are several other minor input differences as listed in Table 1. McLain using DOE-2.1A and Arumi-Noe using DEROB both used the experimentally derived infiltration algorithm, whereas BLAST and DOE-2.1C were run with an available algorithm that approximates the infiltration calculation recommended by the experimenters.

The floor and roof R-values all varied slightly, but because of the extensive insulation levels in these two components, the effect of the input differences is likely to be very small.

COMPARISON OF EXPERIMENTAL AND MODELING RESULTS

The hourly heating load, interior temperature, and wall heat flux were compared for three measuring periods, as well as the cumulative heating load for four- to twelve-day periods.

By asking the modelers to examine detailed hourly output parameters (loads, temperatures, and fluxes), a grid of cross-checks evolved. These were thought to reduce the likelihood of two or more offsetting errors resulting in small cumulative heating load differences between measurements and model predictions, which might be interpreted as consistency.

Cumulative Heating Loads

Figure 7 shows the cumulative heating load comparisons of the four modeling efforts for three periods of time: midwinter (Jan. 12–20, 1982), late winter (Feb. 28–March 10, 1982), and spring (May 25–June 5, 1982) for two test buildings (an 11 in [27.9 cm] adobe, and a 2 in. x 4 in [3.8 cm x 8.9 cm] insulated wood-frame). For each period, the measured value is shown along with the relative performance of BLAST, DOE-2.1A, DOE-2.1C, and DEROB. In order to make the comparison on an absolute basis, the differences were normalized to account for small differences in the comparison period.

The intention is not to compare models but to look for inconsistencies in measured data. The models seem to predict about 10% above measured loads for the massive cell and 10% below what was measured for the frame cell. The percentage differences between model and measured are placed above each bar in Figures 8 and 9. The modelers thus seem to predict loads equally well for the two buildings. Note that this is consistent with the energy balances of the two buildings in Figures 2 and 3. The percentage errors in the spring are large compared to the winter periods; however, the absolute values are more than an order of magnitude smaller than those in the winter period. The conclusion of all four analysts are that the heating load measurements are reproducible within the most likely experimental measuring error.

Interior Temperatures

Each of the analysts compared interior temperatures differently. They all plotted hourly measurements vs. predicted to determine whether the overall behavior of the measurements and model outputs tracked each other. From there they based their quantitative analysis on different measurements and used different statistical parameters.

McLain, using DOE-2.1, chose to use identity plots and then determined correlation coefficients for measured vs. predicted interior air temperature as shown in Figure 8. The least squares comparison of measured and predicted building interior air temperatures (mid-plane average near the wall) produced correlation coefficients for the massive cell of 0.76, 0.84, and 0.91 for the midwinter, late winter, and spring periods. For the frame cell, the same values are 0.89, 0.92, and 0.97. The horizontal temperature stratification is greater in the colder weather periods in the massive building; this apparently gives DOE-2.1A more difficulty in predicting the interior air temperatures under the modeling assumptions used to simulate the heater operation.

Carroll, using BLAST, compared mean interior surface temperatures of all four walls. The average difference for the massive building is 0.3 F (0.17°C), 0.5 F (0.28°C), and 3.1 F (1.71°C) for the midwinter, late winter and spring; for the frame building, the corresponding values are 0.8 F (0.44°C), 0.5 F (0.28°C), and -0.7 F (0.39°C). Except for the massive building in the spring season, BLAST predicts the surface temperatures well within the measurement accuracy.

Birdsall, using DOE-2.1C, had not made any cumulative statistical comparison; however, he did supply a few hourly comparison plots, which suggest that DOE-2.1C does adequately model the springtime floating behavior in both the frame and massive buildings, as shown in Figure 9.

Arumi-Noe, using DEROB, concludes that the horizontal stratification was very likely a correct observation (Arumi-Noe 1984). In the massive cell, the external zone in the DEROB model is consistently lower than the plenum temperature; this is the same as in the measured data. However, the DEROB values are consistently about 2 F (1.11°C) lower than the experimental values. For the insulated stud wall DEROB predicts the cell air temperature within 0.5 F (0.28°C).

Three of the modelers were able to reproduce average interior temperatures measured at mid-plane one foot from the four external walls. Since the BLAST model was set up with constant air temperature of around 69 F (10.6°C) and a very tight floating range, the average air temperature was not compared with the measured data because of the belief that they were in error.

Wall Heat Flux

The least squares correlation coefficients of the DOE-2.1A average hourly heat flux predictions and measurements for the massive building are 0.87, 0.93, and 0.84 for the midwinter, late winter, and spring measuring periods, respectively. For the insulated frame, the correlation coefficients for measured vs. DOE-2.1A heat flux predictions are 0.95, 0.98, and 0.9. The analysts believe the prediction of heat flux in the frame cell is better than in the adobe structure with low R-value walls because the model uses a constant interior film coefficient, which, in reality, varies, therefore creating a larger error in walls with less overall thermal resistance. A second contributing factor to the difficulty in predicting heat flux is the variability of the interior air temperature, which results in varying complex convective loops over time. However, this analysis of the heat flux data did not indicate any basic discrepancies in the data.

Carroll, using BLAST, compared cumulative heat flux values for each one- to two-week test period. The percent differences between measured and predicted for the massive cell are 18.9%, 18.6%, and -132.7%, respectively, for midwinter, late winter, and spring, and for the frame cell the same values are 33%, 30.2%, and -168.6%. It is the belief of the authors that the overprediction of the heat flux in part is due to the fact that a too-high interior air temperature at the walls was assumed in the model.

Effect of Envelope Thermal Mass

One of the major results of the experimental data and analysis is that the measured thermal mass effect, reflected in annual energy use, is 2% to 4% less than a frame, windowless test house with the same R-value. This conclusion was checked using DOE-2.1B by predicting the test cell behavior on an annual basis. For this comparison between a frame and adobe cell, the adobe cell was insulated on the exterior to the same thermal resistance of 10.16 h·ft^2·F/Btu (1.79 m^2·°C/W) measured on the frame cell. One air change per hour was assumed and Albuquerque, New Mexico, typical meterological year (TMY) weather data were used. Results of these simulations are summarized in Table 2. The column titled "Change from Frame" reflects the thermal mass effect, showing a 5.2% annual effect.

A second experimentally observed phenomenon supported by Table 2 is that the prediction of the thermal mass effect by the model appears in the transition months, not during periods when no floating occurs in the frame building as illustrated by the performance in January.

CONCLUSIONS

Despite the problematical thermal behavior within these test buildings and input differences between models, comparison of the cumulative measured versus model predictions of loads generally falls within ±10% for one- to two-week periods. Consistency checks of cumulative load comparisons were made simultaneously with hourly comparisons of measured versus predicted hourly heat flux, air temperature and loads. Multiple model output parameter comparisons with measured data provide a matrix of cross-checks that tend to flush out offsetting errors that could lead to the illusion that the models accurately track building thermal behavior.

The simple 20 ft (6.1 m) by 20 ft (6.1 m) test cells with no windows, no doors, and well-insulated roof and floors are not simple to model. The principal reason is that the lack of detailed measurements on distribution of plenum air and natural convection within the test buildings creates uncertainty in how to best model the interior conditions. A second uncertainty surfaced due to the one-dimensional heat flow constraint in most commonly used mainframe building simulation computer models. One-dimensional heat flow covers most of the major heat paths in typical building envelopes, but not edge losses. These 20 ft (6.1 m) by 20 ft (6.1 m) by 8 ft (1.4 m) test cells have an edge-length-to-floor-area ratio twice that of a conventional 1500 ft^2 residence. A third problem arising in these test buildings, designed to highlight the effect of exterior envelope thermal mass, is caused by the relative importance of film coefficients in low R-value walls. The inside and outside film coefficients, although experimentally measured to some extent, vary continuously and are difficult to model.

The highest correlation coefficients (0.85 to 0.90) occurred when comparing measured to predicted hourly values for wall heat flux. This suggests that the dynamic one-dimensional heat flow through massive and frame wall envelope components can be accurately modeled. The hourly heat loads and interior temperatures are more sensitive to the heat flows that were not as accurately characterized in the model, such as interior airflows and edge losses. The finding supports modelers' claims that their models are reasonable for relative comparisons that mask uncertainties but are not necessarily suitable for absolute annual load predictions.

The experimental results suggest that the maximum benefit of exterior thermal mass in the SWTMS test cells is 2% to 4% annual heating energy savings, despite the location of the test site, which tends to accentuate the effect: high insolation, large ambient temperature fluctuations, heavily insulated ceilings and floors, and low R-value walls. This finding suggests that the dominant impact of mass is not due to the conduction time lag of heat flux nor heat flux amplitude reduction through opaque walls; rather, it is the interior coupling with the inside space resulting in daytime heat storage and evening heat rejection back into the space. This is supported by the modeling sensitivity studies, which show considerably larger energy savings of mass placed on the inside of insulation compared to outside.

The fundamental experimental observation that an exterior envelope mass has an influence during those periods when the outside air temperature swings above and below the building balance temperature in one diurnal cycle is supported by the models. The observation that mass has no influence on daily energy use during the very cold periods when some heating is needed each hour is also confirmed by the computer models.

REFERENCES

Arumi-Noe, Francisco. 1984. Data Consistency Study of the New Mexico Test Cells, prepared for Oak Ridge National Laboratory, draft report (September).

Birdsall, Bruce. 1985. Southwest Thermal Mass Study Cell Comparison Using DOE 2.1C, draft report (January).

Carroll, William; Mertol, Atila; and Sullivan, Robert. Thermal Mass: A Comprehensive Residential Analysis, Lawrence Berkeley Laboratory, draft Interim Report #LBL-18010.

Courville, G. E. and Christian, J. E. 1983. Thermal Mass Program Plan for Thermal Mass in Building Envelopes, Oak Ridge National Laboratory, draft report (March).

Gustinis, John and Robertson, David K. 1981. SWTMS: Construction and Instrumentation Phase, subcontract report prepared by New Mexico Energy Research and Development Institute (NMERDI) (October).

Gustinis, John and Robertson, David K. 1984. The Effect of Envelope Thermal Mass on the Heating Energy Use of Eight Test Buildings in a High Desert Climate, subcontract report prepared by NMERDI, ORNL/Sub/80-7948/1 (April).

McLain, H., Christian, J. E., Ohr, S. Y., and Bledsoe, J. L., Simulation of the SWTMS Test Cells Using the DOE 2.1A Model, draft report, August 1984.

Robertson, David K., Observation and Prediction of the Heating Season Thermal Mass Effect for Eight Test Buildings With and Without Windows, subcontract report prepared by NMERDI, ORNL/Sub/80-7948/2, September 1984.

TABLE 1

Model Input Assumptions

Parameter		DOE-2A	BLAST	DEROB	DOE-2C
1. # Zones		1	1	2	1
2. Conditioning of zones near walls		100% of plenum air	100% of plenum air	Unconditioned, coupled with plenum	100% of plenum air
3. Inside air T		Uniform: Avg. of air temp. near walls	Uniform: plenum T	Nonuniform:	Uniform: Avg. of air temp. near walls
4. Thermostat set point interior control temp		Based on regression	Plenum temp	Constant 69.1 in zone 1	64 F deadband +5° throttling range
5. Wall interior surface film coefficient (Btu/h•ft^2•F)		1.47 (.8)[a]	.54+ X[b]	d	1.47 (.8)[a]
6. Wall exerior surface film coefficient (Btu/h•ft^2•F)		1.80 + 0.244* (W.S.)	1.8 +.244* (W.S.)	d	1.8 + .244* (W.S.)
7. Surface-to-surface wall R (h•ft^2•F/Btu (final runs)	Bldg.[c]				
	1	1.99	1.93	3.08	1.99
	7	10.16	9.78	11.2	10.16
8. Wall density (LBM/CF) (final runs)	Bldg.[c]				
	1	117	80	90	117
	7	14.6	17.216	15.2	14.6
9. Wall Cp (Btu/LBM•F) (final runs)	Bldg.[c]				
	1	0.22	.22	0.24	.22
	7	0.22	.238	.27	.22

TABLE 1 Continued

Parameter	DOE-2A	BLAST	DEROB	DOE-2C
10. Infiltration model	Exper. Derived	Approx. exper. Derived	Exper. Derived	Approx. exper. Derived
11. Weather data	Actual site	Actual site	Actual site	Actual site
12. Internal loads	Exper. measured	Exper. measured	Exper. measured	Exper. measured
13. Roof R ($h \cdot ft^2 \cdot F/Btu$)	30.31	33.17	33.43	30.31
14. Floor ctr. loss R ($h \cdot ft^2 \cdot F/Btu$)	15.35	14.4	12.25	15.35
15. Ground T for floor ctr. loss (F)	Exper. measured	Exper. measured	Exper. measured	Exp. measured
16. Floor edge losses	Not included	Not included	Not included	Not included
17. Wall solar absorptivity	.78	.78	.78	.78

[a]0.8 Btu/$h \cdot ft^2 \cdot F$ is the radiative component of the lumped radiation and convection film coefficient of 1.47 in DOE-2.1.

[b]BLAST uses a constant .54 Btu/$h \cdot ft^2 \cdot F$ for the convective coefficient and calculates each hour the radiative film coefficient.

[c]1 = adobe; 7 = wood-frame.

[d]DEROB calculates heat transfer coefficient each hour.

TABLE 2

DOE-2.1 Comparison of Insulated SWTMS Test Buildings:
1 Air Change per Hour Infiltration
Albuquerque TMY Weather (McLain et al. 1984)

	Insulated Frame			Insulated Adobe				
Month	Load (10^6 Btu)	T_{ave} (F)	% Hours Floating	Load (10^6 Btu)	T_{ave} (F)	% Hours Floating	Change from Frame (10^6 Btu)	(%)
J	2.392	69.14	0.0	2.392	69.14	0.0	0.000	0.0
F	1.933	69.19	2.8	1.926	69.15	0.0	0.003	0.2
M	1.638	69.48	10.5	1.638	69.18	0.5	0.000	0.0
A	0.811	70.24	30.6	0.711	69.25	7.4	-0.100	-12.3
M	0.261	74.76	69.6	0.147	73.28	73.0	-0.144	-43.7
J	0.028	78.85	91.5	0.000	77.30	100.0	-0.028	-100.0
J	0.000	84.77	100.0	0.000	84.55	100.0		
A	0.000	82.08	99.7	0.000	82.24	100.0		
S	0.060	75.72	85.8	0.000	75.93	100.0	-0.060	-100.0
O	0.522	72.07	49.7	0.317	70.30	53.2	-0.205	-39.3
N	1.428	69.32	8.6	1.383	69.19	0.0	-0.045	-3.2
D	2.242	69.15	0.5	2.208	69.15	0.0	-0.034	-1.5
Annual	11.313		46.1	10.730		44.8	-0.583	-5.2

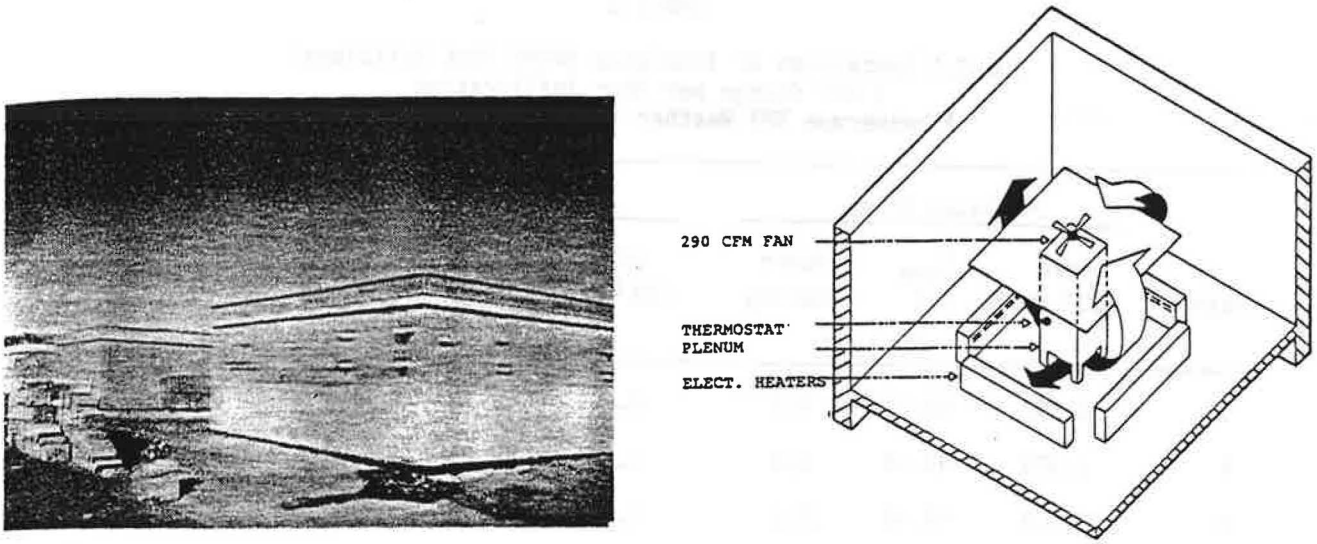

Figure 1. Picture of test buildings with cutaway showing typical heating system

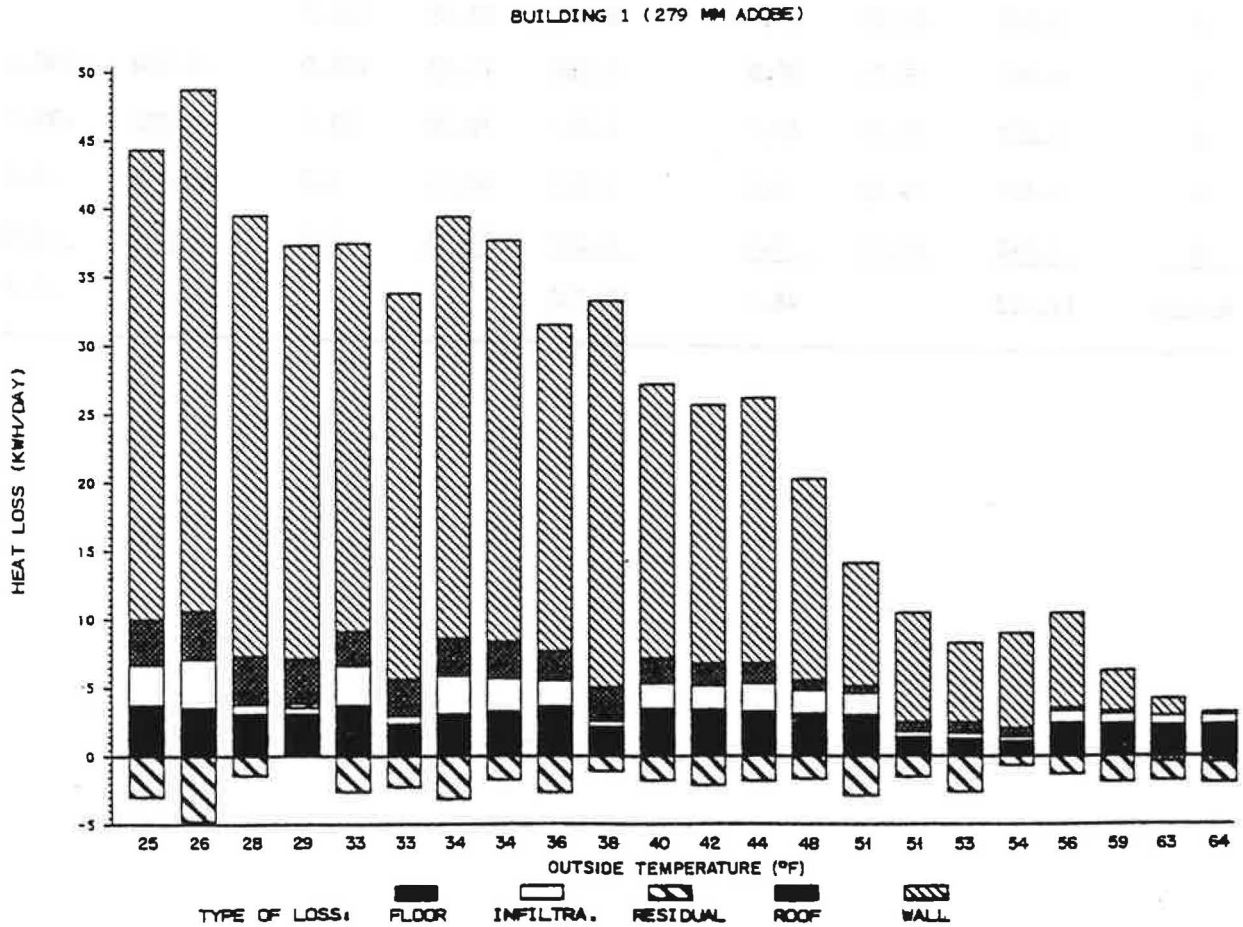

Figure 2. Energy balance for adobe test building

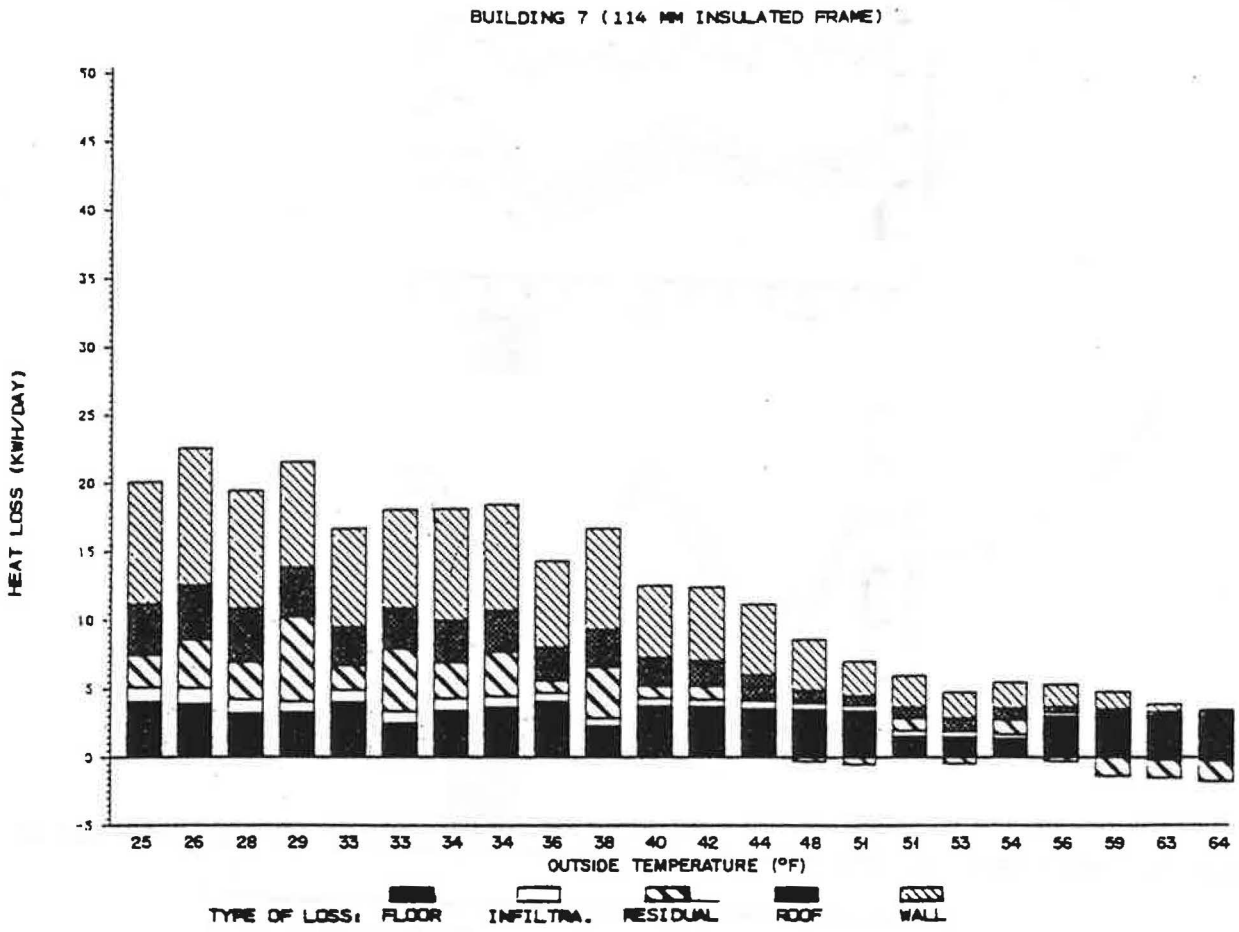

Figure 3. Energy balance for wood-frame test building

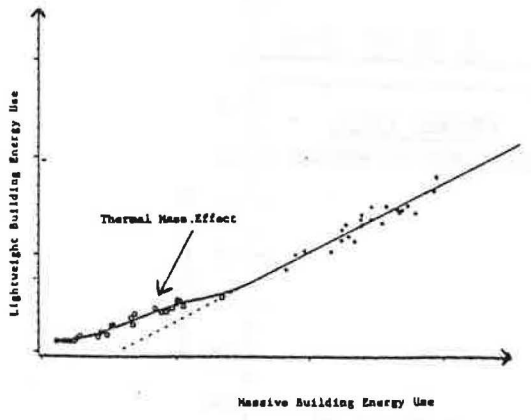

Figure 4. Data plot showing thermal mass effect

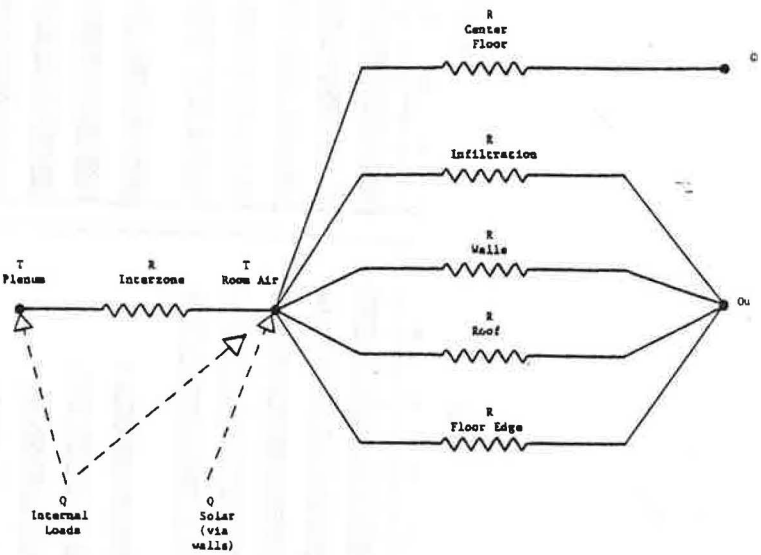

Figure 5. Schematic of building heat loss

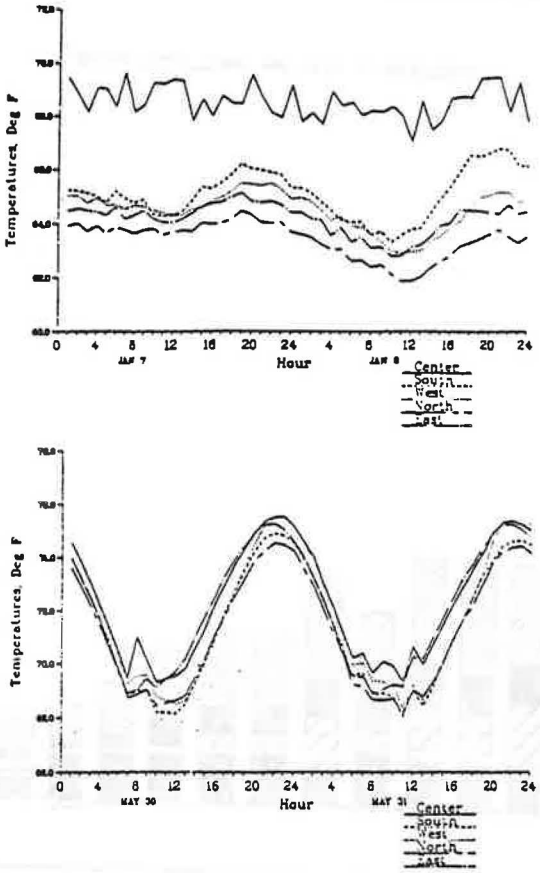

Figure 6. Adobe test building measured interior air temperatures for mid-winter and spring

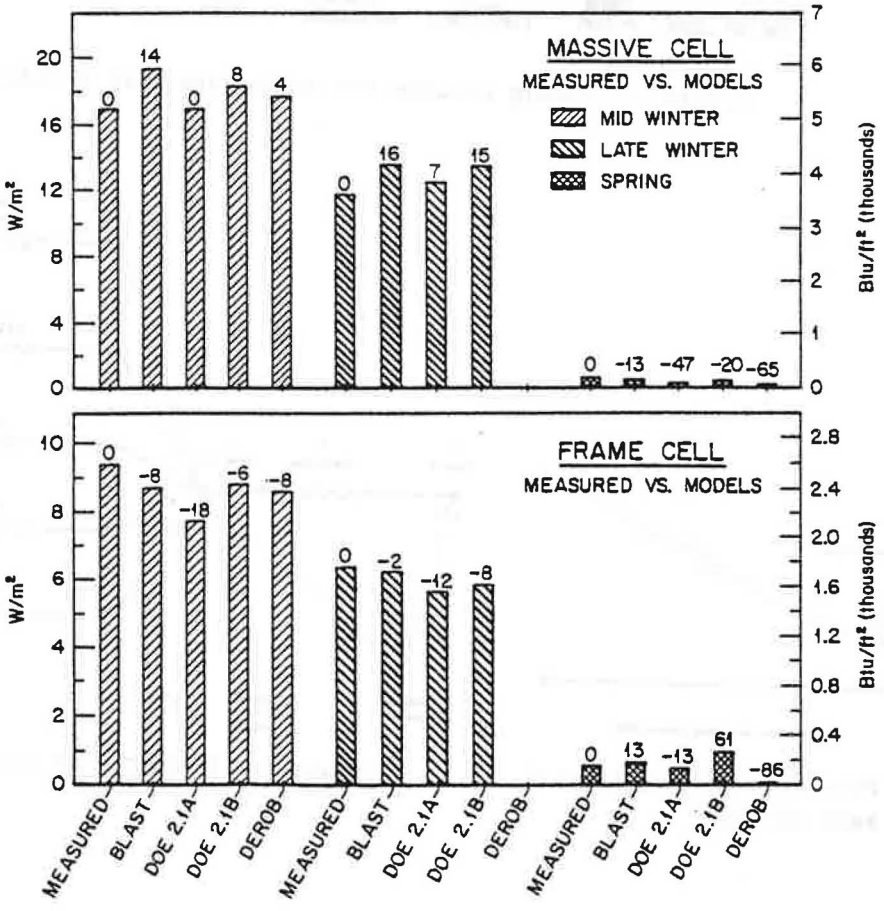

Figure 7. Measured cumulative heating load vs. predicted for adobe and wood-frame test buildings

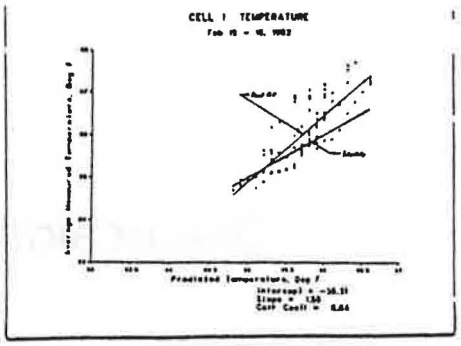

(a) Temperature Least Squares Comparison

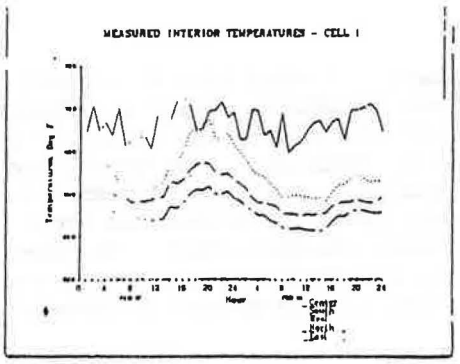

(b) Measured Interior Temperatures

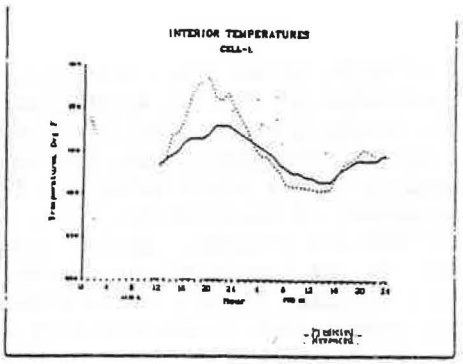

(c) Direct Interior Temperature Comparison

Figure 8. Comparison of DOE-2.1A predicted and measured interior air temperature for test building during mid-winter

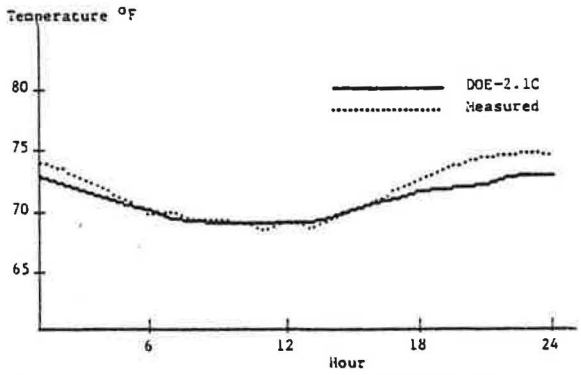

a. Summer — Floating, May 31, 1982, 63.7°F average OA temperature.

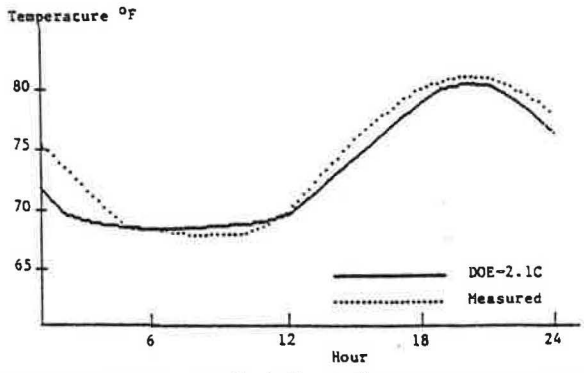

b. Summer — Floating, May 31, 1982, 63.7°F average OA temperature.

Figure 9. Comparison of DOE-2.1C predicted and measured interior air temperature for and wood-frame test buildings during spring

Discussion

G. PROSKIN, Unies Ltd., Winnipeg, Manitoba, Canada: I would like to comment on your observation of thermal stratification in the test buildings. Based on similar experiences with actual houses, I believe that stratification (horizontal and vertical) is a major factor in determining actual heat losses in many types of buildings. Our experiences in trying to simulate annual loads using the HOTCAN energy analysis program has shown that the program has a tendency to overpredict, often badly, in poorly insulated houses and those with poor heat distribution systems. Either situation can produce stratification. In effect, the "surface film" on the inside of the envelope may be, from a thermal perspective, several feet thick and not a fraction of an inch as assumed. Casual observations of actual temperature profiles in such houses tend to confirm such a theory.

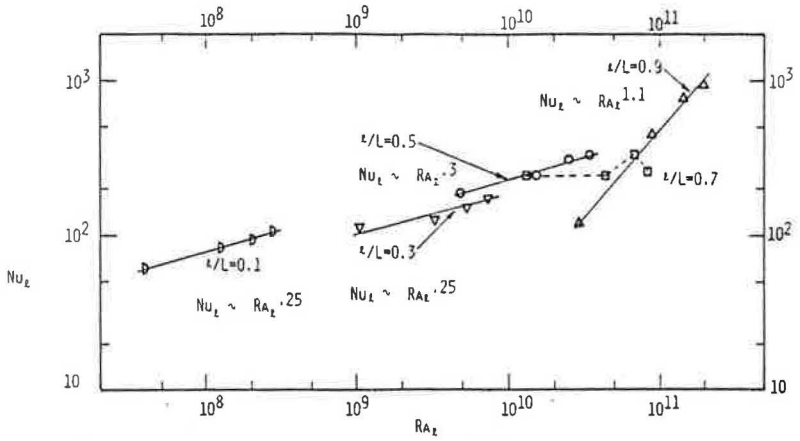

Fig. 8 Variation of local Nusselt number with local Rayleigh number at various heights (ℓ/L) for the constrained cavity

velocities in a region immediately below the shear layer. The constraining flap has caused a significant reduction in the momentum of the exiting flow, with a decrease in the maximum exiting velocity from $u/u_c = .130$ to $u/u_c = .073$ for the low Rayleigh number case and from $u/u_c = .116$ to $u/u_c = 0.5$ for the high Rayleigh number case.

The constrained profiles show similar trends to those found in the unconstrained profiles for the high and low Rayleigh number cases. That is, for the high Rayleigh number case, most of the incoming flow occurred between $y/Y = .036$ and $y/Y = .230$. Velocities below this region were unresolvable by the LDV and appeared to be slightly negative, or to fluctuate about zero. Notice that integration of the velocity profile at any aperture plane is meaningless because of the three-dimensional characteristics of the flow.

For the low Rayleigh number case, small incoming velocities of $u/u_c = .002$ to .003 were measured from $y/Y = .3$ down to $y/Y = .95$. This requires a significant amount of exiting flow to be present at other planes in the cavity width to satisfy continuity, again pointing out the three-dimensional aspects bf the flow. Note that the low Rayleigh number unconstrained cavity flow also demonstrated incoming velocities in the lower aperture region, and this effet does not appear to be as strong for the high Rayleigh number flows.

A complex velocity profile can be observed in Fig. 7(*b*). The upper portion corresponds to the hot boundary layer flow that penetrated the thermocline and moves along the top wall. The lower portion is characteristic of the shear layer, which is felt even close to the hot plate. A similar inflection in the velocity at $y/Y = .275$ was observed at $x/X = .75$, which indicates a horizontal entraining velocity from the aperature to the heated plate. Furthermore, flow visualization outside of the cavity showed that the incoming velocity was also traveling following a horizontal trajectory. As indicated, there is evidence of movement throughout the entire cavity with some small regions remaining almost stagnant. This has an effect in the heat transfer coefficient as will be discussed next.

4.2.2 The Nusselt Number. The local Nusselt numbers are plotted on Fig. 8 as a function of the local Rayleigh number. The results except near the top are almost identical to those of the unconstrained case. The total heat flux to the vertical wall was measured for the constrained and unconstrained apertures for four different wall temperatures. The results indicated a reduction of about 10 percent in the constrained case. This reduction is surprisingly small and could be attributed to the high Pr of the fluid. The slopes of the Nusselt numbers are also almost identical to those of Fig. 5.

It is expected that the heat transfer will be further reduced using smaller and/or off-centered apertures. However, this reduction will be limited because of the ability of the boundary layer flow (due to its large momentum) to penetrate and disrupt the thermocline.

Acknowledgment

Financial support for this research was provided by the U.S. Department of Energy under contract No. DE-AC01-79-ET21105.

References

1 Ostrach, S., "Natural Convection in Enclosures," *Advances in Heat Transfer*, Vol. 8, 1972, p. 161.

2 Buchberg, H., Catton, I., and Edwards, D. K., "Natural Convection in Enclosed Spaces — A Review of Application to Solar Energy Collection," ASME JOURNAL OF HEAT TRANSFER, Vol. 98, 1976, pp. 182–188.

3 Bauman, F., Gadgil, A., Kammerud, R., and Greif, R., "Buoyancy-Driven Convection in Rectangular Enclosures: Experimental Results and Numerical Calculations," ASME Paper 80-HT-66, July 1980.

4 Quon, C., "High Rayleigh Number Convection in an Enclosure — A Numerical Study," *The Physics of Fluids*, Vol. 15, No. 1, 1972, p. 12.

5 Abrams, M., and Greif, R., "A Simple Theory for Predicting the Natural Convective Energy Loss from Side-Facing Solar Cavity Receivers," SAND 81-8201, Jan. 1981.

6 Ku, A. C., Doria, M. L., and Lloyd, J. R., "Numerical Modeling of Unsteady Buoyant Flows Generated by Fire in a Corridor," *Proceedings of the 16th Symp. (Intl) on Combustion*, Cl, 1976, pp. 1373–1384.

7 LeQuere, P., Humphrey, J. A. C., and Sherman, F. S., "Numerical Calculation of Thermally Driven Two-Dimensional Unsteady Laminar Flow in Cavities of Rectangular Cross Section," *Numerical Heat Transfer*, Vol. 4, 1981, pp. 249–283.

8 Department of Energy Solar Central Receiver Semiannual Meeting, Report No. SAND 80-8049, Jan. 1981, issued by Sandia National Laboratories.